Modeling of Magnetoelectric Effects in Composite structures by FEM-BEM coupling

Alberto Urdaneta-Calzadilla, Olivier Chadebec, Nicolas Galopin, Innocent Niyonzima, Gerard Meunier, Bertrand Bannwarth

Modeling of Magnetoelectric Effects in Composite structures by FEM-BEM coupling

Alberto Urdaneta-Calzadilla, Olivier Chadebec, Nicolas Galopin, Innocent Niyonzima,
Gerard Meunier, Bertrand Bannwarth
Univ. Grenoble Alpes, CNRS, Grenoble INP, G2Elab, F-38000 Grenoble, France

In this paper, a coupling of the Finite Element Method (FEM) and the Boundary Element Method (BEM) is used to model the behavior of magnetoelectric effects in composite structures. This coupling of numerical methods makes it possible not to have to consider a free space domain, and thus to use a single mesh for the magnetic, mechanical and electrical problems. This results in a consequent reduction of the number of unknowns which is accompanied by shorter computation times compared to a classical FEM approach. A mixed magnetic vector potential, reduced magnetic scalar potential formulation is used for the magnetic problem, and classical FEM formulations are used for electrical and mechanical problems. The resulting global algebraic system is solved by a block Gauss-Seidel solver.

***Index Terms*—FEM-BEM coupling, magnetoelectric, piezoelectricity, piezomagnetism, multiphysics, Gauss-Seidel method**

I. Introduction

Without relying on induction, electromagnetic coupling can be obtained through the mechanical association of piezoelectric and magnetostrictive materials. The resulting composite structure displays an extrinsic magnetoelectric effect [1] and can allow for magnetic to electric energy conversion or vice-versa. For the modelling of magnetoelectric composites, the FEM allows solving for the behavior of materials with non-trivial structures [2]. Nevertheless, a classical FEM approach has several disadvantages. A free space domain has to be considered to properly model the decay of magnetic fields at infinity, and the extent of this domain is dependent on the distance between the field sources and the active materials. A FEM-BEM coupling for the magnetic phenomena based on a mixed formulation of the magnetic problem [3] can be applied to the modelling of the multiphysics phenomena arising in magnetoelectric composite structures, thus allowing not to explicitly consider a free space region. The magneto-electric problem is then decomposed into three sub-problems: a magnetic problem solved using the FEM-BEM approach, and an electrical and a mechanical problem solved using classical FEM formulations. This coupling of numerical methods introduces resolution difficulties that can be overcome by using a block Gauss-Seidel type solving algorithm.

After introducing the used behavioral laws and the chosen formulation for each single-physics problem, we will compare our magneto-mechanical formulation to an analytical solution. We will then introduce our multiphysics solver and study its convergence for a simple test case.

II. Behavioral laws

Magnetoelectic composites involve piezoelectric and magnetostrictive materials characterized by strong electro(magneto)-mechanical coupling. Piezoelectric materials can be described by a set of linear relationships between the electrical and mechanical quantities [4]. This is not the case for magnetostrictive materials, which generally exhibit non-linear behavior. However, it is possible to induce a polarization state by applying a magnetic field and/or a mechanical prestress and thus define a set of linear relationships [5]. In this framework, the mechanical, electrical and magnetic behavior relations are written:

$$\begin{cases} \boldsymbol{T} = \boldsymbol{c}^{\boldsymbol{E},\boldsymbol{B}} : \boldsymbol{S} - {}^{\mathrm{t}}\boldsymbol{e} \cdot \boldsymbol{E} - {}^{\mathrm{t}}\boldsymbol{h} \cdot \boldsymbol{B}, & (1) \\ \boldsymbol{D} = \boldsymbol{e} : \boldsymbol{S} + \boldsymbol{\varepsilon}^{\boldsymbol{S}} \cdot \boldsymbol{E}, & (2) \\ \boldsymbol{H} = -\ \boldsymbol{h} : \boldsymbol{S} + \boldsymbol{\nu}^{\boldsymbol{S}} \cdot \boldsymbol{B}, & (3) \end{cases}$$

where $\boldsymbol{T}$, $\boldsymbol{S}$, $\boldsymbol{D}$, $\boldsymbol{E}$, $\boldsymbol{B}$ and $\boldsymbol{H}$ are, respectively, the stress tensor, the linear strain tensor, the electric flux density, the electric field, the magnetic flux density and the magnetic field. $\boldsymbol{c}^{\boldsymbol{E},\boldsymbol{B}}$ is the stiffness tensor at constant electric field and magnetic flux density, $\boldsymbol{\varepsilon}^{\boldsymbol{S}}$ is the electrical permittivity tensor at constant strain, $\boldsymbol{\nu}^{\boldsymbol{S}}$ is the magnetic reluctivity tensor at constant strain, $\boldsymbol{e}$ is the piezoelectric tensor and $\boldsymbol{h}$ the piezomagnetic tensor. As we are describing heterogeneous composite structures, the piezoelectric tensor $\boldsymbol{e}$ is taken null in the piezomagnetic phase and, reciprocally, piezomagnetic tensor $\boldsymbol{h}$ is taken equal to zero in the piezoelectric phase.

III. Electro-Magneto-Mechanical Modeling

We consider an open boundary domain $\Omega = \Omega_0 \cup \Omega_{pe} \cup \Omega_{pm}$ where Ω_0, Ω_{pe} and Ω_{pm} represent the free space, the magnetostrictive and the piezoelectric domains, respectively, as shown in Figure (1). We will also call $\Omega_m = \Omega_{pe} \cup \Omega_{pm}$ the domain of active materials. The magnetoelectric problem consists in solving Maxwell's equations in the framework of quasistatic regime [6]:

$$\boldsymbol{\nabla}\times\boldsymbol{E} = 0, \quad \boldsymbol{\nabla}\cdot\boldsymbol{D} = 0, \quad \boldsymbol{\nabla}\times\boldsymbol{H} = \boldsymbol{J_s}, \quad \boldsymbol{\nabla}\cdot\boldsymbol{B} = 0 \quad \text{in } \Omega, \tag{4}$$

as well as the balance of linear momentum for the mechanical equilibrium without body force:

$$\boldsymbol{\nabla} \cdot \boldsymbol{T} = 0 \quad \text{in } \Omega_m. \tag{5}$$

A. Magnetic problem

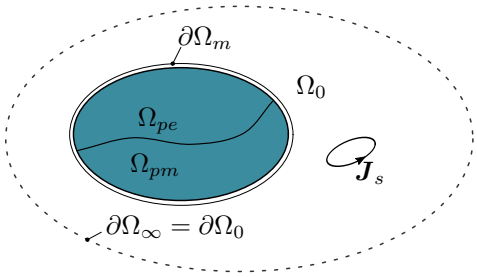

Fig. 1. Domains of the magnetic problem. With $\boldsymbol{J_s}$ a prescribed solenoidal current density and Ω_0 an open boundary domain.

To derive a variational formulation inside the active material domain Ω_m in terms of the magnetic vector potential $\boldsymbol{a}$ ($\boldsymbol{B} = \boldsymbol{\nabla} \times \boldsymbol{a}$), considering the absence of electric current in Ω_m, we multiply (4), Maxwell-Ampere equation (4), by the test function $\boldsymbol{\delta a}$. After integration by parts, it follows:

$$\int_{\Omega_m} \boldsymbol{\nabla} \times \boldsymbol{\delta a} \cdot \boldsymbol{H}\ d\Omega - \int_{\partial\Omega_m} (\boldsymbol{\delta a} \times \boldsymbol{H}) \cdot \boldsymbol{n}\ d\partial\Omega = 0 \,\forall\, \boldsymbol{\delta a}, \quad (6)$$

where $\partial\Omega_m$ is the exterior surface of Ω_m and $\boldsymbol{n}$ the unit outward normal vector to $\partial\Omega_m$. Given the magnetic behavior law (3), we can rewrite the volume term in (6) as:

$$\begin{aligned}\int_{\Omega_m} \boldsymbol{\nabla} \times \boldsymbol{\delta a} \cdot \boldsymbol{H} d\Omega = \int_{\Omega_m} \boldsymbol{\nabla}\times\boldsymbol{\delta a} \cdot \boldsymbol{\nu^S} \cdot \boldsymbol{\nabla}\times\boldsymbol{a}\ d\Omega_m \\ - \int_{\Omega_{pm}} \boldsymbol{\nabla}\times\boldsymbol{\delta a} \cdot\ \boldsymbol{h} : \boldsymbol{S}\ d\Omega_m.\end{aligned} \quad (7)$$

Furthermore, $\boldsymbol{H} = \boldsymbol{H_0} - \boldsymbol{\nabla}\phi_{red}$, with $\boldsymbol{H_0}$ the field created by external currents $\boldsymbol{J_s}$, calculated by the Biot-Savart law, and ϕ_{red} the magnetic reduced scalar potential. After the application of some vector identities applied to the surface term of (6), similarly to [3], the weak form reads: find ($\boldsymbol{a}$, ϕ_{red}) such that:

$$\begin{aligned}\int_{\Omega_m} \boldsymbol{\nabla}\times\boldsymbol{\delta a} \cdot \boldsymbol{\nu^S} \cdot \boldsymbol{\nabla}\times\boldsymbol{a}\ d\Omega_m + \int_{\partial\Omega_m} (\boldsymbol{\nabla} \times \boldsymbol{\delta a}) \cdot \boldsymbol{n}\ \phi_{red}\ d\partial\Omega_m \\ - \int_{\Omega_{pm}} \boldsymbol{\nabla}\times\boldsymbol{\delta a} \cdot \boldsymbol{h} : \boldsymbol{S}\ d\Omega_m = \int_{\partial\Omega_m} (\boldsymbol{\delta a} \times \boldsymbol{n}) \cdot \boldsymbol{H_0}\ d\partial\Omega_m \,\forall\, \boldsymbol{\delta a}.\end{aligned} \quad (8)$$

The discretization of (8) is performed using edge elements for the vector potential $\boldsymbol{a}$ and 0-order surface elements for the reduced scalar potential ϕ_{red}. The previous discretization can take account of a nonlinearity in $\boldsymbol{\nu}^S$.

The behavior of the magnetic field in the free space domain is taken into account by adding an equation to the system. In $\partial\Omega_m$, the potential ϕ_{red} verifies the Laplace equation $\Delta\phi_{red} = 0$ [7]. Green's third identity applied to ϕ_{red} in $\partial\Omega_m$ leads to the following equation [8]:

$$\frac{1}{2}\phi_{red} - \int_{\partial\Omega_m} \phi_{red} \frac{\partial G}{\partial n} d\partial\Omega_m + \int_{\partial\Omega_m} G \frac{B_n}{\mu_0} d\partial\Omega_m = \int_{\partial\Omega_m} G\ H_{0n} d\partial\Omega_m, \quad (9)$$

where G is the Green function of the 3D Laplacian operator.

Using a Galerkin approach. Equation (9) is discretized using 0-order surface elements. As $\int B_n\ dS = \oint\ \boldsymbol{a}^{surf} \cdot \boldsymbol{dl}$, after discretization of (9) the magnetic vector potential in edge elements is introduced in the discretized equation from the flux of the magnetic induction through each facet element.

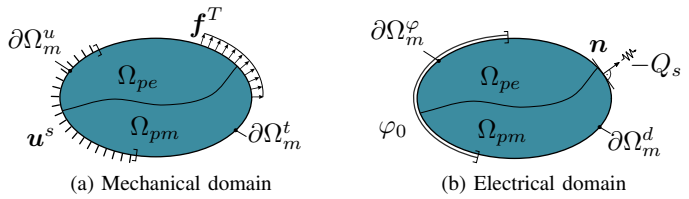

(a) Mechanical domain (b) Electrical domain

Fig. 2. Mechanical and electrical domains. With $\boldsymbol{f}^T$ the surface forces, $\boldsymbol{u}^s$ the imposed displacement, φ_0 the imposed electric potential and Q^s the surface charge density.

B. Electric and mechanical problems

The electrical and mechanical problems are limited to the active material's domain Ω_m (Fig. 2). Indeed, even if a FEM-BEM coupling can also be formulated for the electrical problem, we can neglect the leaks of the electric field for two reasons: the high permittivity of the considered piezoelectric materials channels the fields inside the active domain, and the electrodes exciting the piezoelectric material are in direct contact with the active domain. Thus treating the electric problem with the FEM and only meshing the active region is a reasonable approximation for the modeled phenomena.

From (1) and (5), together with the small strains assumption and neglecting the magnetic forces, we obtain the mechanical weak form [9]: find $\boldsymbol{u}$ such that:

$$\begin{aligned}\int_\Omega \boldsymbol{\delta S} : \boldsymbol{c} : \boldsymbol{S} d\Omega - \int_\Omega \boldsymbol{\delta S} : \boldsymbol{e}^t \cdot \boldsymbol{E} d\Omega - \int_\Omega \boldsymbol{\delta S} : \boldsymbol{h}^t \cdot \boldsymbol{B} d\Omega \\ = 0 \quad \forall \boldsymbol{\delta S}\end{aligned} \quad (10)$$

with $\boldsymbol{u}$ the displacement vector, φ the electric scalar potential and $\boldsymbol{S} = \text{sym}(\boldsymbol{\nabla u})$, $\boldsymbol{E} = -\boldsymbol{\nabla}\varphi$, $\boldsymbol{\delta S} = \text{sym}(\boldsymbol{\nabla \delta u})$ together with the Dirichlet boundary condition on $\partial\Omega_m^u$ (Fig. 2a). We do not impose charges on the electrodes, $Q_s = 0$ on $\partial\Omega^d$, but potentials $\varphi = \varphi_0$ on $\partial\Omega_m^\varphi$, one floating and the other in reference. In these conditions, the electric weak form is: find φ such that:

$$\int_{\Omega_m} \boldsymbol{\nabla}\delta\varphi \cdot \boldsymbol{\varepsilon^S} \cdot \boldsymbol{E}\ d\Omega_m + \int_{\Omega_{pe}} \boldsymbol{\nabla}\delta\varphi \cdot \boldsymbol{e} \cdot \boldsymbol{S}\ d\Omega_m = 0 \,\forall\, \delta\varphi. \quad (11)$$

IV. Matrix system and resolution method

The resulting global matrix system (12) is composed of sparse FEM matrices (in light colors) and full BEM matrices (in dark blue), and has a big scaling difference between coefficients. Usually, a suitable solver is used for each single-physics problem: a preconditioned GMRES iterative solver is appropriate for problems involving full matrices (here the magnetic problem) while the MUMPS direct solver is better suited for problems with sparse matrices (here the electrical and mechanical problems). With these considerations, the system (12) can be solved iteratively using a block Gauss-Seidel scheme (13). Contrary to a direct resolution, the block Gauss-Seidel scheme thus allows using an optimized solver for each sub-system.

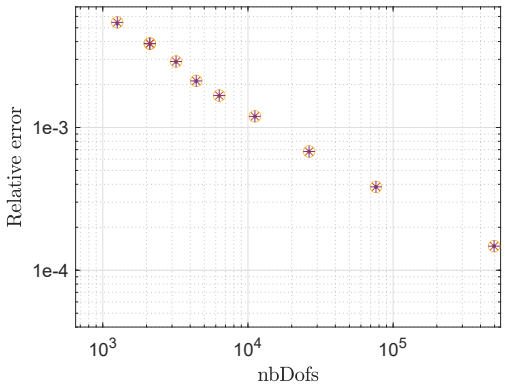

Fig. 3. Convergence of averaged H(z) ('.'), S_{11} ('×'), S_{22} ('o') and S_{33} ('+') on meshed spheres vs analytical solutions.

$$\begin{bmatrix} \underline{\boldsymbol{K}}_{aa} & \underline{\boldsymbol{0}} & \underline{\boldsymbol{K}}_{au} & \underline{\boldsymbol{0}} \\ \underline{\boldsymbol{0}} & \underline{\boldsymbol{K}}_{a\phi} & & \\ \underline{\boldsymbol{0}} & \underline{\boldsymbol{K}}_{G} \; \underline{\boldsymbol{K}}_{\frac{\partial G}{\partial n}} & \underline{\boldsymbol{0}} & \\ \underline{\boldsymbol{K}}_{ua} & \underline{\boldsymbol{0}} & \underline{\boldsymbol{K}}_{uu} & \underline{\boldsymbol{K}}_{u\varphi} \\ \underline{\boldsymbol{0}} & & \underline{\boldsymbol{K}}_{\varphi u} & \underline{\boldsymbol{K}}_{\varphi\varphi} \end{bmatrix} \begin{pmatrix} \underline{\boldsymbol{a}} \\ \underline{\boldsymbol{\phi}}_{red} \\ \underline{\boldsymbol{u}} \\ \underline{\boldsymbol{\varphi}} \end{pmatrix} = \begin{pmatrix} \boldsymbol{Sh}_{mag}^{\Omega_m} \\ \boldsymbol{Sh}_{mag}^{\partial\Omega_m} \\ \boldsymbol{Sh}_{meca} \\ \boldsymbol{Sh}_{elec} \end{pmatrix} \tag{12}$$

$$[\boldsymbol{K}_{ii}]\{\boldsymbol{x}_i^{n+1}\} = \{\boldsymbol{Sh}_i\} - \sum_{j=0}^{i-1}[\boldsymbol{K}_{ij}]\{\boldsymbol{x}_j^{n+1}\} - \sum_{j=i+1}^{n}[\boldsymbol{K}_{ij}]\{\boldsymbol{x}_j^{n}\}. \tag{13}$$

The block Gauss-Seidel scheme also allows for solving well conditioned sub-systems, as extra-diagonal sub-matrices are scaled by the current solutions and introduced as second hand terms (13). The stopping criteria for the multiphysics resolution algorithm was the relative convergence of the single-physics solution between each iteration n.

V. Validation

The magneto-mechanical formulation is validated with respect to an analytical formula for the field and strains, considering an unconstrained sphere under a uniform source field. The magnetic field inside a sphere under a uniform source field is given by:

$$\boldsymbol{H} = \frac{3}{\mu_r + 2}\boldsymbol{H_0}. \tag{14}$$

To obtain a coupled analytical solution for an unconstrained piezomagnetic sphere, we solve for $\boldsymbol{T} = \boldsymbol{0}$ and (14) with $\mu_r = \boldsymbol{B}/(\mu_0 \boldsymbol{H})$. We tested our magneto-mechanical formulation with first-order finite elements, with coefficient similar to [10] and increasingly finely meshed spheres imposing no surface forces and a uniform source field. We obtained the convergence curves presented in Figure 3. We observe the convergence up to 10^{-4} of the FEM-BEM solution towards the analytical solution. Having validated the magneto-mechanical coupling, we will focus on solving the full problem.

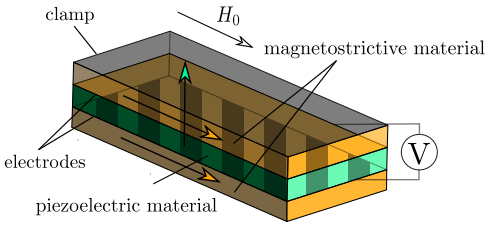

Fig. 4. Three layers magnetoelectric heterostructure, the colored arrows represent the poling direction of the materials.

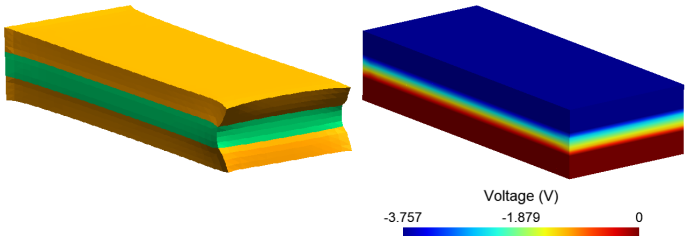

Fig. 5. Amplified displacement field and nodal voltage (V).

VI. Results

The full proposed model was tested on a composite structure with the geometry presented in Figure 4. It is composed of a PZT piezoelectric layer in between two Terfenol-D magnetostrictive layers and dimensions $3{\times}6{\times}14$ mm. The mesh has 5656 elements. The device functions as follows: the source field drives the deformation of the magnetostrictive layers. As both phases are mechanically bonded together, the piezoelectric layer will deform and an electric voltage will appear between the electrodes, as shown in Figure 5.

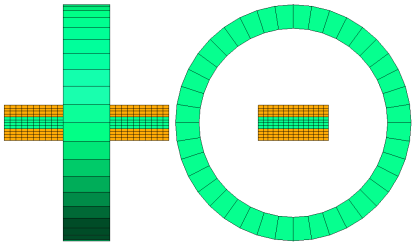

Fig. 6. Coil positioning.

We considered a coil crossed by $100\,A$ as a source for the magnetic excitation and positioned as shown in Figure 6, also, all linear coupling tensors with coefficients from [10]. We obtained, as shown in Figure 5, a deformation of the global structure along its length, and the presence of a static electric potential difference between the electrodes.

VII. Solver behavior

The resolution order of the global matrix at each block Gauss-Seidel iteration remains an open question, and many possibilities arise. In problems driven by a particular physics, and in order to have non-null solutions for the first iterations, a natural resolution order can sometimes be found. For the device in question, the magnetic field drives the deformation of the piezoelectric layer, cf Figure 4, so a natural order of

resolution would be to solve at each Gauss-Seidel iteration for the magnetic problem followed by the mechanical and then the electric problem. Figure 7 gives the convergence ratios, as defined in Figure (7), of the different problems per resolution number.

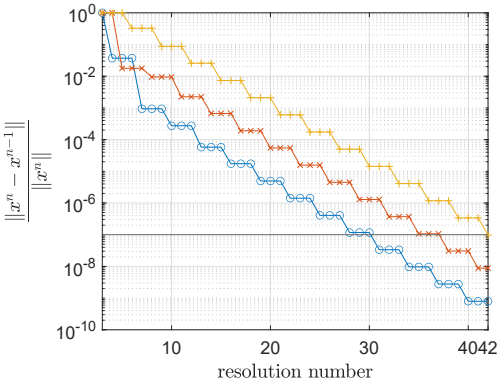

Fig. 7. Convergence ratio of magnetic (o), mechanical (x) and electric (+) solutions after given n° of resolutions for the block Gauss-Seidel algorithm with a 1-2-3-1... resolution pattern for the given mesh. $\|x^n\|$ Relates the nth solution of the given problem.

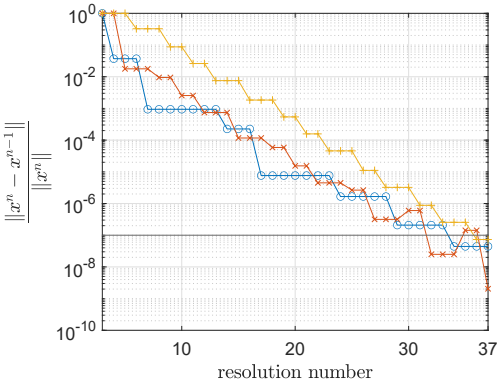

Fig. 8. Convergence ratio of magnetic (o), mechanical (x) and electric (+) solutions after given n° of resolutions with an adaptative resolution pattern for the given mesh.

The resolution pattern of multiphysics problems is an active research subject, for example for the study of fluid-solid interactions, where multiple resolutions in subdomains are performed in order to obtain a coupled solution. In [11], multiple resolution patterns are proposed, and the different physics solved in a previously defined and fixed order within a black-box multiphysics solver.

Another approach to solving the multiphysics problem is to have no imposed resolution order, but after each resolution, to compare the convergence ratios of all single-physics problems and solve for the one with the worst convergence ratio, that has not immediately been solved before. For our particular application, as the magnetic and electric problem are uncoupled, the mechanical problem must be solved at least every two resolutions. This resolution algorithm was implemented, and we obtained the convergence curves presented in Figure 8. They can be compared to the classical Gauss-Seidel presented in Figure 7. As shown in Table I, for this particular application, the adaptative algorithm solves the multiphysics problem in

TABLE I
NUMBER OF RESOLUTIONS NEEDED FOR MULTIPHYSICS CONVERGENCE PER SINGLE-PHYSICS PROBLEM

Problem	regular G-S	adaptative G-S
Magnetic	14	8
Electric	14	14
Mechanical	14	15

37 iterations vs 42 resolutions for the classic algorithm with a tolerance of 10^{-7}. But in our particular implementation, it translated into a total resolution time of $133\,s$ vs $188\,s$ (-29 %) on a personal computer (Intel© Core™ i7-10610U CPU @ 1.80GHz 2.30 GHz), the magnetic problem is indeed particularly difficult to solve as it contains both FEM and BEM matrices. The relative difference between single-physics solutions of the two tested resolution algorithm remained inferior to the tolerance of the solver.

VIII. Conclusion

In this paper, we proposed a FEM-BEM formulation of the magneto-electric effect in composite structures. A mixed formulation of the magnetic phenomena allowed us to use vector shape functions and not to explicitly consider and mesh an air region. The magneto-mechanical model was successfully validated against an analytical solution. We then solved the full magneto-electric problem on an example of composite structure and studied two variations of the block Gauss-Seidel resolution algorithm, one with a fixed resolution pattern and an adaptative one leading to a lesser number of resolutions and a lower resolution time in the studied test case.

References

[1] Y. Cheng, B. Peng, Z. Hu, Z. Zhou, M. Liu, "Recent development and status of magnetoelectric materials and devices," *Physics Letters*, A 382, 2018, 3018–3025. doi:https://doi.org/10.1016/j.physleta.2018.07.014.

[2] T. T. Nguyen, F. Bouillault, L. Daniel, X. Mininger, "Finite element modeling of magnetic field sensors based on nonlinear magnetoelectric effect," *Journal of Applied Physics*, 2011, .doi : 10.1063/1.3553855

[3] Q. Phan, G. Meunier, O. Chadebec, J. Guichon and B. Bannwarth, "BEM-FEM formulation based on magnetic vector and scalar potentials for eddy current problems," *19th International Symposium on Electromagnetic Fields in Mechatronics, Electrical and Electronic Engineering (ISEF)*, 2019, pp. 1-2, doi: 10.1109/ISEF45929.2019.9096899.

[4] H. F. Tiersten, "Hamilton's principle for linear piezoelectric media," in *Proceedings of the IEEE*, 1967, vol. 55, nb. 8, pp.1523-1524, doi: 10.1109/PROC.1967.5887.

[5] G. Engdhal, "Modeling of Giant Magnetostrictive Materials," in *Handbook of Giant Magnetostrictive Materials*. Academic Press, 2000. pp. 127-133.

[6] J. D. Jackson, *Classical Electrodynamics*, 3rd ed. New York, Wiley & Sons, 1999.

[7] J.P.A. Bastos, N. Sadowski, *Electromagnetic Modeling by Finite Element Methods*, 1st ed. CRC Press. 2003.

[8] C.A. Brebbia, S. Walker, *Boundary Element Techniques in Engineering, 1st ed.* Elsevier Science, 1980.

[9] N. Galopin, X. Mininger, F. Bouillault, L. Daniel, "Finite Element Modeling of Magnetoelectric Sensors," *IEEE Trans. Magn.*, vol. 44, no. 6, pp. 834-837, June 2008. doi:10.1109/TMAG.2008.915781

[10] T. A. Do, H. Talleb, A. Gensbittel and Z. Ren, "Homogenization of Magnetoelectric 0–3 Type Composites by 3-D Multiphysics Finite-Element Modeling," *IEEE Trans. Magn.*, vol. 55, no. 6, pp. 1-4, June 2019, Art no. 7401004, doi: 10.1109/TMAG.2019.2900149.

[11] B. Uekermann, B. Gatzhammer, M. Mehl, "Coupling Algorithms for Partitioned Multi-Physics Simulations," in *Informatik 2014*, Plödereder, E., Grunske, L., Schneider, E. & Ull, D. (Hrsg.), Bonn, Gesellschaft für Informatik e.V., pp. 113-124.